Observation of a Zundel-like transition state during proton transfer in aqueous hydroxide solutions

Sean T. Roberts[a], Poul B. Petersen[a], Krupa Ramasesha[a], Andrei Tokmakoff[a,1], Ivan S. Ufimtsev[b,2], and Todd J. Martinez[b,2]

[a]Department of Chemistry, Massachusetts Institute of Technology, Cambridge, MA 02139; and [b]Department of Chemistry, University of Illinois at Urbana–Champaign, Urbana, IL 61801

Edited by Graham R. Fleming, University of California, Berkeley, CA, and approved June 11, 2009 (received for review February 11, 2009)

It is generally accepted that the anomalous diffusion of the aqueous hydroxide ion results from its ability to accept a proton from a neighboring water molecule; yet, many questions exist concerning the mechanism for this process. What is the solvation structure of the hydroxide ion? In what way do water hydrogen bond dynamics influence the transfer of a proton to the ion? We present the results of femtosecond pump-probe and 2D infrared experiments that probe the O-H stretching vibration of a solution of dilute HOD dissolved in NaOD/D_2O. Upon the addition of NaOD, measured pump-probe transients and 2D IR spectra show a new feature that decays with a 110-fs time scale. The calculation of 2D IR spectra from an empirical valence bond molecular dynamics simulation of a single NaOH molecule in a bath of H_2O indicates that this fast feature is due to an overtone transition of Zundel-like $H_3O_2^-$ states, wherein a proton is significantly shared between a water molecule and the hydroxide ion. Given the frequency of vibration of shared protons, the observations indicate the shared proton state persists for 2–3 vibrational periods before the proton localizes on a hydroxide. Calculations based on the EVB-MD model argue that the collective electric field in the proton transfer direction is the appropriate coordinate to describe the creation and relaxation of these Zundel-like transition states.

Grotthuss mechanism | 2D infrared spectroscopy

Proton transfer in water is the process at the heart of biological redox chemistry and energy conversion processes such as photosynthesis and cellular respiration (1). Although its extraordinary speed and efficiency has generally been attributed to the rearrangement of O-H bonds that effectively move the charge rather than a specific proton, the water structure around the charge defect and the mechanism of translocation remain challenging to study experimentally. Researchers commonly discuss the solvated excess proton in terms of 2 limiting structures, the Eigen cation (2), a triply solvated hydronium ion ($H_3O^+ \cdot 3H_2O$), and the Zundel ion (3), a proton equally shared between 2 water molecules ($H_5O_2^+$ or $H_2O \cdot H \cdot OH_2^+$). However, the difference in energy between these 2 configurations is small, on the order of the energy of a hydrogen bond (2–3 kcal/mol) (4), which allows these structures to interconvert on femtosecond to picosecond time scales (5, 6). Thus, to meaningfully address the structure of the excess proton, one must also consider its dynamics. Similar questions related to this view of aqueous proton transfer (PT) exist for the hydroxide ion, whereby proton transfer occurs from water to OH^-. What are the ion's limiting structures, and in what manner do changes in the water structure influence the ion's structural diffusion?

Initial proposals for transport of the hydroxide ion described the process as the mirror image of that observed in acids (7) and postulated the existence of a stable $H_3O_2^-$ state (8). Ab initio simulations (9–11) suggest a different scenario in which the oxygen of the ion primarily accepts 4 hydrogen bonds and the loss of 1 of these allows the hydroxide ion to accept a proton. Neutron scattering experiments (12, 13) measure a hydroxide coordination number between 3 and 4 but are unable to view time-dependent changes in this value. Ultrafast spectroscopy has been used to characterize the time scales for hydroxide reorientation and hydrogen bond relaxation, but these studies remain difficult to interpret in terms of the underlying structural evolution (14, 15).

We present the results of femtosecond pump-probe (PP) and 2D infrared spectroscopy (2D IR) measurements of a dilute solution of HOD dissolved in NaOD/D_2O solution. Upon the addition of NaOD, a new spectral feature appears that relaxes on a 110-fs time scale. The calculation of spectra from a recently developed empirical valence bond molecular dynamics (EVB-MD) simulation model of aqueous NaOH suggests that the observed spectral feature arises from Zundel-like states, wherein a proton is delocalized between a water molecule and the hydroxide ion. Comparison of the measured relaxation time scale and estimates of the frequency of vibration of shared protons indicate that this state exists transiently for 2–3 vibrational periods during the transfer of the proton. Electric field fluctuations are suggested to play a role in the creation of these Zundel-like states and the translocation of the hydroxide ion.

Infrared Spectroscopy of Isotopically Dilute Hydroxide

The O-H stretching vibration of an HOD molecule dissolved in D_2O is a sensitive reporter of changes in the hydrogen bonding environment near the proton (16–18). The formation of a hydrogen bond pulls on the O-H bond, broadening its stretching potential and decreasing its vibrational frequency, ω_{OH}. The wide breadth of the absorption line shape (Fig. 1) is indicative of the large distribution of hydrogen-bonding environments present in the liquid. By exciting molecules within the absorption line shape with temporally short infrared pulses and then watching how their frequencies change with time, we can observe the evolution of water's hydrogen-bonding structure.

Upon the addition of NaOD, the O-H stretching peak broadens significantly to low frequency. This broadening is similar to changes that occur in the spectra of H_2O upon the addition of strong acids or bases, which show a continuum absorption that spans the entire midinfrared spectrum and features a strong enhancement in the frequency region below the O-H stretch (3). This continuum absorption is attributed to protons shared between 2 oxygen atoms whose stretching potentials are rapidly modulated by changes in the local solvent environment. Also observed with increasing NaOD concentration is the appearance of a peak at 3600 cm^{-1}. Although only a shoulder in the infrared spectra, Raman spectra of alkali hydroxides show this as a strong and sharp scattering peak that arises from the OH^- stretch (19, 20). Because of the negative charge on the hydroxide ion, its

Author contributions: S.T.R. and A.T. designed research; S.T.R., P.B.P., K.R., and I.S.U. performed research; S.T.R., I.S.U., and T.J.M. contributed new reagents/analytic tools; S.T.R. and A.T. analyzed data; and S.T.R. and A.T. wrote the paper.

The authors declare no conflict of interest.

This article is a PNAS Direct Submission.

[1]To whom correspondence should be addressed. E-mail: tokmakof@mit.edu.

[2]Present address: Department of Chemistry, Stanford University, Stanford, CA 94305.

This article contains supporting information online at www.pnas.org/cgi/content/full/0901571106/DCSupplemental.

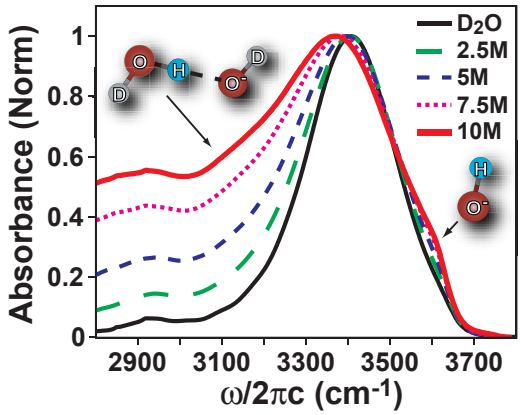

Fig. 1. FT-IR spectra of ≈1% HOD in varying concentrations of NaOD/D_2O with the D_2O background subtracted. Spectra are normalized to the absorption maximum. As the NaOD concentration increases, a new feature appears at 3,600 cm^{-1} because of the OH^- stretch, and a strong broadening appears at low frequency because of HOD molecules hydrogen bonded to OD^- ions.

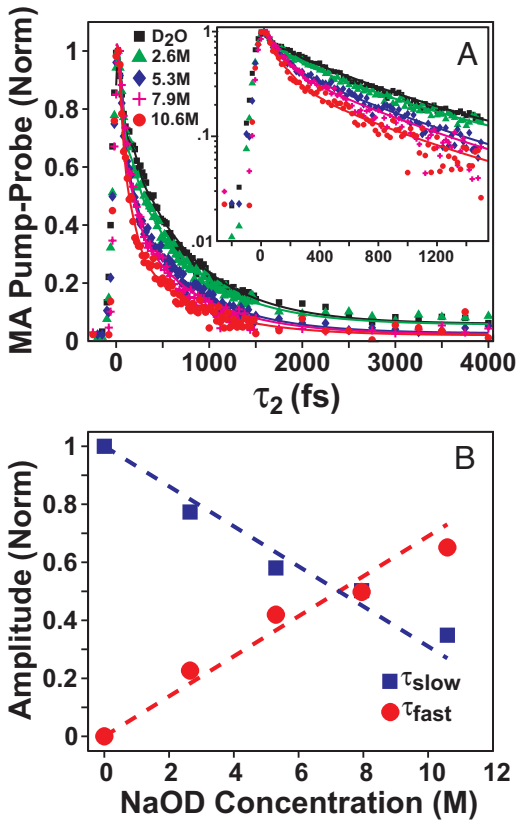

Fig. 2. Pump-probe transients of the O-H stretching region for differing concentrations of NaOD/D_2O. (*A*) Pump-probe decay traces and biexponential fits. As the NaOD concentration decreases, the measured decay acquires a fast component of 110 fs. (*B*) Relative amplitudes of the fast and slow decay components to the PP signal.

proton can only act as a weak hydrogen bond donor (12, 13) leading to a blue shift of its O-H stretching frequency relative to that of a HOD molecule hydrogen bonded to D_2O.

As an initial test of how water dynamics change upon the addition of NaOD, we performed PP transient absorption measurements of the O-H stretching transition using 45-fs pulses with 350 cm^{-1} bandwidth centered at 3,325 cm^{-1}. In concentration-dependent studies, the addition of deuteroxide leads to a fast decay component whose amplitude grows monotonically with hydroxide concentration (Fig. 2). Each of the decay traces can be fit well by a biexponential function with time constants of 710 and 110 fs. The long time constant is similar to what has been previously measured for OH vibrational relaxation of HOD in D_2O (21–24). The fast time constant was hinted at in transient hole-burning measurements of concentrated deuteroxide solution, where a decay on the order of the experimental time resolution, ≈160 fs, was observed (15).

To better understand the origin of the 110-fs decay, we carried out 2D IR measurements of the O-H stretching transition as a function of NaOD concentration. 2D IR is well suited to the study of short-lived species that arise and disappear during PT because it combines the time resolution needed to observe transient species with the necessary spectral resolution to isolate their signals. In a 2D IR measurement, a series of femtosecond pulses infrared pulses drive the O-H vibrations of the sample and stimulate the emission of a signal field that is interferometrically characterized. The Fourier transform 2D IR spectrum is related to the joint probability of exciting a molecule with initial frequency, ω_1, and detecting that molecule at a different frequency, ω_3, after a waiting period τ_2 (25, 26). In a typical experiment, at small values of τ_2, a diagonally elongated line shape is expected because molecules have not had time to sample their environments and lose memory of their initial excitation frequencies. As τ_2 increases, the excitation and detection frequencies lose correlation, and a circular line shape is observed. For weakly anharmonic vibrational transitions, peaks in 2D IR spectra appear as doublets, consisting of a positive peak due to the photobleach of the $v = 1 \leftarrow 0$ fundamental transition and a negative anharmonically shifted peak along the ω_3 axis due to photoinduced absorption of the $v = 2 \leftarrow 1$ transition.

Two-dimensional IR spectra as a function of both waiting time and NaOD concentration were acquired [see supporting information (SI)]. Of these, spectra for 10.6 M NaOD and neat HOD/D_2O are shown in Fig. 3*A*. Strong off-diagonal broadening of the spectra whose amplitude scales with NaOD concentration is observed at short values of τ_2 at all probed frequencies. As τ_2 increases, this broadening disappears, relaxing completely within ≈100 fs (Fig. 3*B*). This collapse of intensity with τ_2 is the opposite of what is expected in 2D exchange experiments. Off-diagonal intensity is also observed in a 2D IR spectrum when a coupling between oscillators exists; however, given that the solution under investigation is isotopically dilute, the probability of 2 separate O-H oscillators encountering each other is small. Instead, the large broadening observed at early waiting times shows that a subset of OH vibrations samples the entire probed frequency range within a few tens of femtoseconds. Furthermore, the fast relaxation of the off-diagonal intensity occurs on a time scale similar to that observed in the PP measurements. This indicates that the broad off-diagonal component observed at early times in the 2D IR data are the same as that giving rise to the fast decay component observed in the PP measurements.

Different scenarios for the rapid spectral relaxation can be put forward. A fast decay component has previously been observed in IR transient hole-burning measurements of isotopically dilute hydroxide solutions (15). The authors of ref. 15 hypothesized that as a deuterium atom is transferred back and forth between an OD^- ion and a D_2O molecule, the hydrogen bonds of the remaining spectator water molecules in the OD^- solvation shell will be rapidly modulated, leading to the observed relaxation. A second explanation is that the spectral feature arises from transferring protons themselves as the O-H stretching potential flattens during PT, causing a large decrease in ω_{OH}. Such spectral evolution of shared protons has been invoked as an explanation for the absorption continua in IR spectra of strong acids and bases (3).

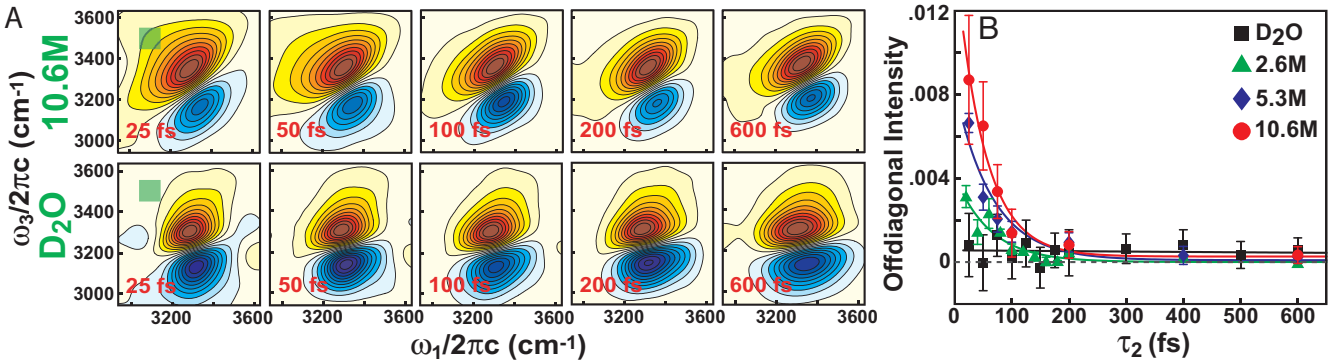

Fig. 3. Summary of experimental 2D IR spectra as a function of NaOD concentration and waiting time. (*A*) Two-dimensional spectra of HOD in 10.6M NaOD and D_2O. (*A*) Two-dimensional IR spectra for 10.6 M NaOD and neat HOD/D_2O as a function of waiting time. At early waiting times a large off-diagonal broadening is observed that quickly relaxes as τ_2 increases. (*B*) The integrated area ω_1 = 3,050–3,150 cm^{-1} and ω_3 = 3,450–3,550 cm^{-1} normalized by the integrated absolute value spectrum at the earliest recorded waiting time. The integrated region is highlighted by the green box overlaid on the τ_2 = 25-fs spectra.

Another explanation, which we provide evidence for, recognizes that as the O-H stretching potential broadens during PT, transitions from the ground state to higher lying vibrational states can move into resonance with the probing pulses. A continuum of rapidly evolving structures with different proton potentials will allow a continuum of excitation pathways involving these states to contribute to the measured 2D IR spectra. Given that the $v = 2 \leftarrow 0$ transition of the shared proton stretch of the $H_3O_2^-$ ion in the gas phase is predicted to appear as low as 1,718 cm^{-1} (27) and that a nonlinear scaling of the O-H transition dipole with frequency is known to occur (28, 29), it is reasonable that overtone transitions of such Zundel-like species absorb strongly in the frequency range of our experiments.

Modeling Based on Empirical Valence Bond MD Simulations

Comparison between simulation and experiment provides a means to test this hypothesis and interpret the experimental results in atomistic detail. A number of methods have been developed for the calculation of nonlinear infrared signals from classical MD simulations, many of which have been applied to the study of aqueous hydrogen bond dynamics (30). However, no standard methodology yet exists for the calculation of spectra for reactive systems such as the one studied here. To aid in the determination of the origin of the relaxation behavior of the 2D IR spectra, we have devised a method of calculating nonlinear signals from a recently developed EVB-MD simulation model of aqueous NaOH. This model is an extension of a recently developed classical simulation model in which the negative charge of the OH^- ion is spread over a ring 1.3 Å in diameter (31). The EVB-MD model gives an average first solvation shell size of 3.8 water molecules, consistent with the value of 3.9 derived from neutron scattering results (13).

The methodology we have developed for the calculation of vibrational frequencies is derived from semiempirical cluster-based mapping methods used in simulations of HOD/D_2O (32). Electronic structure calculations are used to map the quantum mechanical O-H stretching frequency onto a collective coordinate that can be calculated from the simulation at each time step. From instantaneous MD configurations, we select a cluster containing an HOD molecule and 16–18 surrounding D_2O molecules and then stretch the O-H bond using DFT calculations [Gaussian 98: B3LYP 6–311+G(d,p)]. Vibrational frequencies and transition dipole moments for transitions involving $v = 0$–4 are obtained from the 1D O-H stretching potential traced out by this procedure. Although the simulation dynamics are propagated with an entirely protonated sample, in constructing clusters, we assume that one of the hydrogen atoms is that of an HOD molecule and that all other hydrogens are deuterons.

Recent simulations of a model parameterized to describe PT in a phenol–amine complex dissolved in chloromethane found a 1:1 mapping between the difference in energy of the reactant and product wells of the O-H stretching potential and its vibrational frequencies (33). Fig. 4*A* shows the correlation between the frequency of the $v = 1 \leftarrow 0$ transition, ω_{10}, and the solvent coordinate, ΔE_{sol}, calculated from the 1D potentials derived from the electronic structure calculations. ΔE_{sol} is defined as the difference in energy of the O-H stretching potential evaluated at

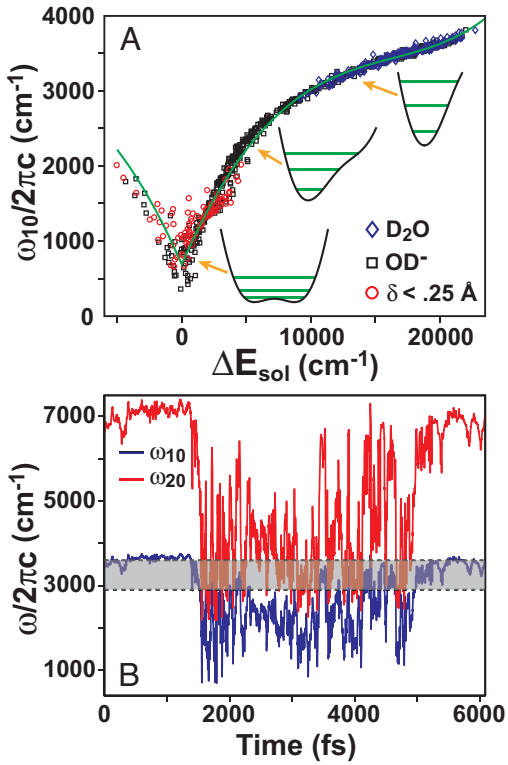

Fig. 4. DFT generated map for the calculation of vibrational frequencies and a representative frequency trajectory. (*A*) Mapping between the solvation coordinate ΔE_{sol} and the fundamental OH frequency ω_{10} calculated from clusters taken from the EVB-MD simulation. For a given $DOH^{\cdots}OD^-$ hydrogen bond, $\delta = |r_{HO} - r_{HO-}|$. An equally shared proton corresponds to $\delta = 0$. (*B*) A ≈6-ps section of a frequency trajectory during which the observed proton partially transfers to the hydroxide ion. During each of the attempted transfer events, the ω_{20} transition moves within the experimentally probed frequency region (gray).

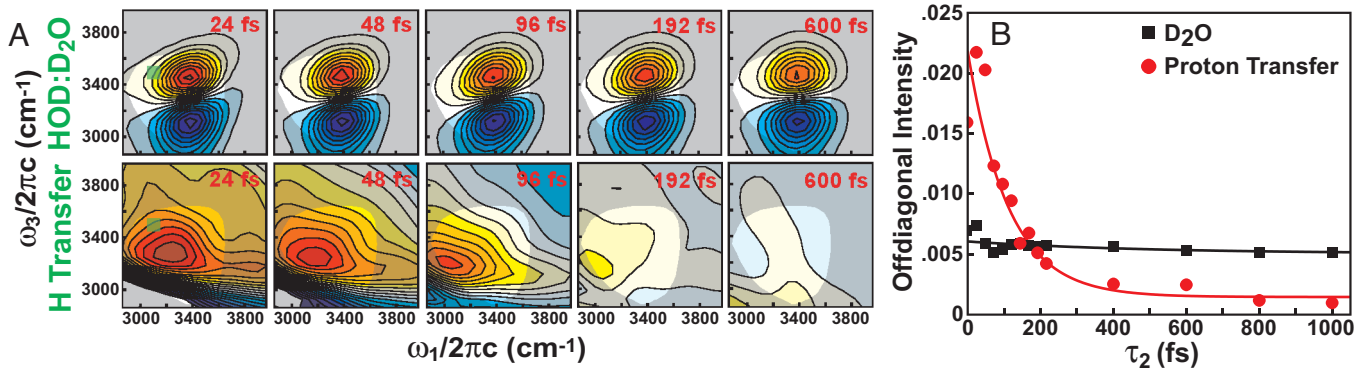

Fig. 5. Summary of 2D IR spectra calculated from the EVB-MD simulation. (*A*) Two-dimensional spectra for HOD molecules that do not encounter the OD^- ion (*Upper*) and for HOD molecules engaging in proton transfer (*Lower*). Contours are plotted relative to the maximum positive signal at $\tau_2 = 0$. The signal for protons in the course of switching appears to completely relax within 200 fs. The shaded region represents the spectral range excluded by the product of the experimental pulse bandwidth in the ω_1 and ω_3 region. (*B*) The off-diagonal intensity for the component spectra shown in *A*. The normalization scheme and integration range are identical to that used in Fig. 3*B*. Spectra were multiplied by the experimental pulse spectrum along both the ω_1 and ω_3 dimensions before integration. A fit to the PT component gives a decay time scale of 110 fs.

2 points, 1.0 and 1.5 Å, which approximate the positions of the 2 minima of the O-H stretching potential for a proton that is strongly shared between 2 oxygen atoms. The mapping between ΔE_{sol} and ω_{10} is found to behave symmetrically about $\Delta E_{sol} = 0$.

Unfortunately, the calculation of ΔE_{sol} with DFT at each simulation time step for a given hydrogen atom is too costly to be practical. As an approximation of ΔE_{sol}, at each time step we stretch the O-H bond and calculate ΔE_{sol} using the EVB potential. Tracing out the full O-H stretching potential in this fashion is inaccurate because the empirical model used for water parameterizes the Lennard–Jones force solely in terms of the oxygen atom positions. Nonetheless, our calculations suggest that although the computation of ΔE_{sol} in this manner is a poor approximation to that derived from DFT, comparison of the 2 quantities shows that they are linearly correlated ($\rho = 0.95$). Vibrational frequencies calculated by using this methodology give a rms error of 54.8 cm^{-1} for HOD molecules hydrogen bonded to D_2O, a comparable level of error to that obtained for a recent electric field-based frequency map for HOD/D_2O (32).

With the methodology in place to calculate vibrational transitions, we can determine the spectral signatures associated with PT events. Fig. 4*B* shows a sample of a frequency trajectory where the HOD molecule undergoes multiple attempted PT events with a neighboring OD^- ion. During these events, ω_{10} is observed to undergo an extremely strong and rapid red shift as the O-H stretching potential broadens. However, as ω_{10} decreases in value, so too do the higher transitions within the vibrational potential. The shaded area of Fig. 4*B* represents the frequency range probed in our 2D IR experiments. During proton transfer events, the direct overtone transition, ω_{20}, moves into this range when the proton becomes shared between the HOD molecule and the OD^- ion. This suggests that excitation pathways exist wherein the first pulse interacts with the $v = 2 \leftarrow 0$ transition of a transferring proton in a Zundel-like state, but because of shifts in the shape of the vibrational potential as the proton localizes, subsequent pulses probe the fundamental transition of the hydroxide- and hydrogen-bonded water.

For a weakly anharmonic system, the transition dipole for the $v = 2 \leftarrow 0$ overtone transition is often orders of magnitude smaller than that of the fundamental. However, the shape of the vibrational potential during PT events is highly anharmonic, leading to a nonlinear dependence of transition dipole intensities on the solvation coordinate (34). When ω_{20} tunes into resonance with the laser in the 2D IR measurement, its transition dipole is $\approx$2/3 that of the fundamental transition at equilibrium (see SI). This supports the hypothesis that excitation pathways involving mixed excitation of the fundamental and overtone transitions will be strong enough to be observed in the 2D IR and PP experiments.

The calculation of 2D IR spectra from fluctuating frequency trajectories by using a semiclassical perturbative approach has been described in refs. 35 and 36. Typically, the calculation of spectra for weakly anharmonic systems neglects 2 quantum transitions, but these transitions are included here to determine their contribution to the measured 2D IR data. To isolate the spectral features due to HOD molecules interacting with D_2O, we identify molecules that remain outside of first solvation shell of both the OH^- and the Na^+ ions for the full simulation run. To identify analogous spectral features for hydrogen atoms in the course of proton transfer, we locate each point in the trajectory where the proton of a water molecule in the OD^- solvation shell becomes equidistant from its own oxygen atom and the OD^- oxygen. By using such a geometric criterion, a number of back transfer events occur. We select against these by only counting a PT event as successful if the next subsequent PT involves a different hydrogen atom. By using such a criterion, 370 individual PT events were identified. Two-dimensional IR spectra of the transferring species are then calculated by evaluating the expressions for the 2D IR response with a time origin that precedes the PT by 1 ps and then stepping the time origin up to the PT.

Fig. 5*A* shows the calculated 2D IR spectral components as a function of τ_2, emphasizing the spectral region probed in our experiments. The component representing HOD/D_2O appears similar to that which has been calculated from classical simulation models (32, 35, 37). The spectra of HOD molecules undergoing PT are quite broad, with positive intensity peaked at 3,300 cm^{-1} but covering the majority of the OH frequency region. Moreover, the PT peak is observed to rapidly decay and has nearly disappeared within 200 fs. Fig. 5*B* compares the integrated intensity of the 2 spectral components in the same off-diagonal region examined in Fig. 3*B*. The HOD/D_2O response shows some changes in this region as the calculated spectra broaden and rotate because of hydrogen bond exchange but remains largely constant. In contrast, the component because of molecules engaging in proton transfer relaxes rapidly with a time constant of 110 fs, consistent with the measured PP data. Because our simulation model does not include any effects due to population relaxation of excited HOD molecules or their reorientation, the calculated decrease in intensity is only the result of ultrafast spectral sweeping.

Using the simulation, we can analyze each quantum mechanical pathway that contributes to the 2D IR line shape to more

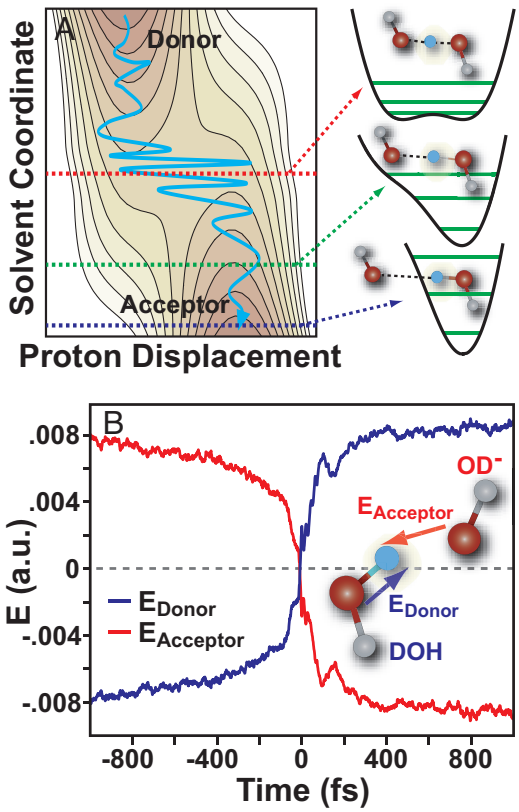

Fig. 6. Collective reaction coordinate for proton transfer. (*A*) Illustration of the free-energy surface for proton transfer suggested by the measured dynamics. The picosecond evolution of a solvent coordinate prepares a Zundel-like state at the saddle point of the potential. Once at this point, multiple recrossing events occur over the course of ≈110 fs before the shared proton forms a stable covalent bond. (*B*) The projection of the electric field along the donor bond that breaks during PT and the acceptor bond that is formed.

finely discern which dynamics are observed in experiment. Rather than spectral evolution of the $v = 1 \leftarrow 0$ excitation, we find that ≈80% of the calculated decrease of off-diagonal intensity is the result of excitation of pathways involving the $v = 2 \leftarrow 0$ transition and its subsequent spectral shifting out of the experimentally accessible frequency window. These calculations suggest that the experimentally observed decay measures how long a delocalized proton in a Zundel-like configuration takes to localize on one of the oxygen atoms.

We have also calculated the spectra of the spectator water molecules hydrogen bound to the OD^- ion about the formation of a Zundel-like state. These spectra, provided in the SI, are somewhat broader but very similar to the bulk water response shown in Fig. 5*A*, indicating that the spectral shifts experienced by spectator water molecules are not significantly different from fluctuations experienced by HOD molecules distant from the ion.

Discussion and Conclusions

Our findings concerning the structural diffusion of the hydroxide ion are consistent with the free-energy surface shown in Fig. 6*A*. The 2 wells on either side of the potential correspond to a proton covalently bonded to a different oxygen atom of an $HO^{\cdots}H^{\cdots}OH^-$ pair and the saddle point in the middle of the surface corresponds to a Zundel-like shared proton. The vertical axis represents a slow solvent coordinate that controls the barrier for the PT reaction. Once the system has evolved to the saddle point, the proton can undergo multiple recrossing events before relaxing into either well. Given the gas-phase value of 697 cm^{-1} for the shared proton stretch of the $H_3O_2^-$ ion (38) (vibrational period of 49 fs), we can estimate a lower bound of 4.6 for the average number of times that the proton crosses the saddle point (2.3 vibrational periods) before localizing on a particular oxygen. This compares well with the value of 5.9 obtained from the EVB-MD simulation.

The potential shown in Fig. 6*A* represents a view of PT in hydroxide solutions very similar to that found by Car–Parrinello MD simulations. These simulations found 2 principal time scales that contribute to the proton transfer rate, a fast time scale of 180 fs that corresponds to "proton rattling" events in which the proton returns to the original oxygen atom after a series of PT events within a Zundel-like state, and a slower 1.7-ps process that acts to gate the formation of a Zundel-like configuration (10). Given that the simulations use a fully deuterated bath, the time scale for proton rattling agrees well with our experimentally observed value of 110 fs. The identity of the slow solvent coordinate that gates the structural diffusion of the OD^- ion was found to be the number of hydrogen bonds accepted by the ion, which oscillates between 3 and 4 (9, 10). Proton transfer events involving a 4-coordinate hydroxide ion were found to be rare because the water molecule created in such an exchange would accept 3 hydrogen bonds. The rate-limiting step for PT is postulated to be the breakage of a hydrogen bond to the OD^- ion, which symmetrizes the transition state and allows PT.

In the EVB-MD simulation, we find some support for this mechanism. During PT, the average solvation shell size decreases from ≈3.66 to 3.26. However, the observation that the solvation shell does not decrease uniformly to 3, reflects the fact that ≈25% of the PT events occur from 4-coordinate states in this simulation model. This suggests that although the coordination number of the hydroxide ion is correlated with PT events, it may not be the best reaction coordinate. Because the vibrational spectroscopy of the proton is inseparable from the proton transfer coordinate, a meaningful variable would describe both.

Simulations of autoionization in water have found that this process is driven by strong transient electric fields (39) arguing that molecules outside of the first solvation shell play a role in PT. Zundel has also proposed that the motion of a proton between a donor and acceptor molecule responds adiabatically to fluctuations of the electric field because of the surrounding solvent (3). In addition, our spectral calculations show that the frequency of the O-H stretching transition is well correlated with proton exchange events. At frequencies ≥3,000 cm^{-1}, a near 1:1 correlation between the O-H stretching frequency and the projection of the collective electric field because of the surrounding solvent molecules along the O-H bond is found (18). These observations argue that the collective electric field coordinate serves to describe both the OH spectroscopy and the PT reaction.

Fig. 6*B* plots the projection of the electric field onto the shifting proton along the donor and acceptor O··H bonds due to all molecules within the simulation box but excluding the field contributions from the donor and acceptor atoms. About PT events, the total field projected along these directions changes sign, implying that the solvent is rearranging in such a way as to destabilize the donor bond in favor of the acceptor bond. In this model, the fluctuating field is a better predictor of proton transfer events than 4-to-3 coordinate switching, although these processes will naturally be correlated because the first solvation shell of the hydroxide ion and the proton donor necessarily make the largest contributions to the fields. In addition, the recent findings that water structure reorganizes in concerted hydrogen bond rearrangements that lead to large electric field shifts (18, 24, 40) suggests that these same hydrogen bond dynamics are dominant contributors to the field during proton transfer events.

To summarize, our results show the fleeting existence of Zundel-like $H_3O_2^-$ states that arise in the course of structural diffusion of the hydroxide ion. Spectral signatures of these states were found by using 2D IR and PP spectroscopy. The develop-

ment of a methodology to calculate vibrational frequencies for the reactive system studied here from an EVB-MD simulation model allowed confirmation of the spectral assignments. Once formed, these states persist for only 2–3 vibrational periods before forming a new hydrogen bond. The transient nature of these states suggests that the motion of the proton is coupled to the surrounding solvent environment through dielectric fluctuations that originate in hydrogen bond rearrangements.

Materials and Methods

Samples. Stock solutions of 2.6, 5.3, 7.9, and 10.6 M NaOD were prepared by dilution of a 40% NaOD solution (99.5% deuteration; Cambridge Isotope Laboratories) with D_2O. A small amount of H_2O was then added to give an absorbance no greater than 0.3. The amount of H_2O needed to achieve this was ≈1% of the solution volume. Solutions were held between two 100-nm-thick Si_3N_4 windows (Norcada) within a Teflon sample cell with a path length of 100 μm. The Si_3N_4 windows were found to give no nonresonant signal when the 3 excitation pulses overlap.

Pump-Probe Acquisition. Pump-probe experiments were performed by using 45-fs pulses with 350 cm^{-1} of bandwidth centered at 3,325 cm^{-1}. The polarization of each beam was controlled with $\lambda/2$ wave plates (Alphalas) and wire-grid polarizers (Molectron). The pump was oriented at the magic angle (54.7°) with respect to the probe to remove effects due to the reorientation of molecules. The probe was passed through an analyzing polarizer and a narrow band filter (FWHM ≈50 cm^{-1}) centered at 3,400 cm^{-1} after the sample to reduce interference with the $v = 2 \leftarrow 1$ transition. To reduce noise from fluctuations of the pump intensity, a weak reflection of the pump pulse before the sample was used for shot-to-shot normalization.

Two-Dimensional IR Acquisition. Similar to the PP measurements, the pulses used for the 2D IR experiments were 45 fs in duration and centered at 3,350 cm^{-1}. Spectra were recorded at ZZZZ (parallel) polarization. The design of the interferometer used for the measurements has been described in ref. 41. In lieu of time–frequency detection using a spectrometer and IR array detector, surfaces were measured in the time domain by scanning the local oscillator stage at constant velocity while stepping τ_1 for rephasing and nonrephasing experiments. The value of τ_3 for each laser shot was determined by making use of the He/Ne tracer that copropagates with the infrared pulses for alignment purposes. The tracer of the third excitation pulse and that of the local oscillator were overlapped after the sample and their interference was detected in quadrature. Unwrapping of the He/Ne phase allowed accurate determination of τ_3. After the signal and local oscillator are combined on a beam splitter, both the transmitted and reflected signal–local oscillator pairs are measured and differenced for balanced detection. With such a procedure, a single 2D IR surface for a given waiting time can be obtained within ≈8 min. The spectra shown in Fig. 2*A* are the average of between 2 and 5 surfaces collected in the time domain that were separately Fourier transformed before averaging.

Simulation Methodology. The MD simulation was performed on a single Na^+ OH^- ion pair solvated by 214 H_2O molecules in a cubic box with periodic boundary conditions (density = 1.01 g/cm^3) by using the MS-EVB model developed from a classical simulation model of aqueous NaOH (31). The system was equilibrated for 100 ps by using velocity rescaling ($T = 303 \pm 8$ K) before making a production run 900 ps in length in the NVE ensemble with the velocity Verlet integrator and a 0.5-fs time step. Ewald summation was used to account for long-range electrostatic forces. The kinetic energy was rescaled every 10 ps to compensate for minor energy drift. This energy rescaling does not disturb the dynamical properties of the system over the time scale of interest.

ACKNOWLEDGMENTS. We thank Ward Thompson for suggesting use of the solvation coordinate for the mapping of vibrational frequencies. This work was supported by U.S. Department of Energy Grants DE-FG02-99ER14988 (to A.T.) and DE-FG02-05ER46260 (to T.J.M.) and the American Chemical Society Petroleum Research Fund (A.T.). P.B.P. acknowledges fellowships from the Carlsberg Foundation and the Camille and Henry Dreyfus Foundation.

1. Ball P (2008) Water as an active constituent in cell biology. *Chem Rev* 108:74–108.
2. Eigen M (1964) Proton transfer, acid–base catalysis, and enzymatic hydrolysis. *Angew Chem Int Ed* 3:1–19.
3. Zundel G (2000) Hydrogen bonds with large proton polarizability and proton transfer processes in electrochemistry and biology. *Adv Chem Phys* 111:1–217.
4. Agmon N (1995) The Grotthuss mechanism. *Chem Phys Lett* 244:456–462.
5. Marx D, Tuckerman ME, Hutter J, Parrinello M (1999) The nature of the hydrated excess proton in water. *Nature* 397:601–604.
6. Markovitch O, et al. (2008) Special pair dance and partner selection: Elementary steps in proton transport in liquid water. *J Phys Chem B* 112:9456–9466.
7. Agmon N (2000) Mechanism of hydroxide mobility. *Chem Phys Lett* 319:247–252.
8. Asthagiri D, Pratt LR, Kress JD, Gomez MA (2004) Hydration and mobility of HO^-(aq). *Proc Natl Acad Sci USA* 101:7229–7233.
9. Tuckerman ME, Chandra A, Marx D (2006) Structure and dynamics of OH^-(aq). *Acc Chem Res* 39:151–158.
10. Chandra A, Tuckerman ME, Marx D (2007) Connecting solvation shell structure to proton transport kinetics in hydrogen-bonded networks via population correlation functions. *Phys Rev Lett* 99:145901.
11. Tuckerman ME, Marx D, Parrinello M (2002) The nature and transport mechanism of hydrated hydroxide ions in aqueous solution. *Nature* 417:925–929.
12. Botti A, Bruni F, Imberti S, Ricci MA (2003) Solvation of hydroxyl ions in water. *J Chem Phys* 119:5001–5004.
13. Botti A, Bruni F, Imberti S, Ricci MA, Soper AK (2004) Ions in water: The microscopic structure of concentrated NaOH solutions. *J Chem Phys* 120:10154–10162.
14. Thøgersen J, Jensen SK, Petersen C, Keiding SR (2008) Reorientation of hydroxide ions in water. *Chem Phys Lett* 466:1–5.
15. Nienhuys H-K, Lock AJ, van Santen RA, Bakker HJ (2002) Dynamics of water molecules in an alkaline environment. *J Chem Phys* 117:8021–8029.
16. Moller KB, Rey R, Hynes JT (2004) Hydrogen bond dynamics in water and ultrafast infrared spectroscopy: A theoretical study. *J Phys Chem A* 108:1275–1289.
17. Lawrence CP, Skinner JL (2003) Vibrational spectroscopy of HOD in D_2O III. Spectral diffusion, and hydrogen-bonding and rotational dynamics. *J Chem Phys* 118:264–272.
18. Eaves JD, Tokmakoff A, Geissler P (2005) Electric field fluctuations drive vibrational dephasing in water. *J Phys Chem A* 109:9424–9436.
19. Walrafen GE, Douglas RTW (2006) Raman spectra from very concentrated aqueous NaOH and from wet and dry, solid, and anhydrous molten, LiOH, NaOH, and KOH. *J Chem Phys* 124:114504.
20. Corridoni T, Sodo A, Bruni F, Ricci MA, Nardone M (2007) Probing water dynamics with OH^-. *Chem Phys* 336:183–187.
21. Gale GM, et al. (1999) Femtosecond dynamics of hydrogen bonds in liquid water: A real time study. *Phys Rev Lett* 1068–1071.
22. Nienhuys HK, Woutersen S, Santen R A v and Bakker HJ (1999) Mechanism for vibrational relaxation in water investigated by femtosecond infrared spectroscopy. *J Chem Phys* 111:1494–1500.
23. Loparo JJ, Fecko CJ, Eaves JD, Roberts ST, Tokmakoff A (2004) Reorientational and configurational fluctuations in water observed on molecular length scales. *Phys Rev B* 70:180201.
24. Fecko CJ, Loparo JJ, Roberts ST, Tokmakoff A (2005) Local hydrogen bonding dynamics and collective reorganization in water: Ultrafast IR spectroscopy of HOD/D_2O. *J Chem Phys* 122:054506.
25. Jonas DM (2003) Two-dimensional femtosecond spectroscopy. *Annu Rev Phys Chem* 54:397–424.
26. Cho M (2008) Coherent two-dimensional optical spectroscopy. *Chem Rev* 108:1331–1418.
27. McCoy AB, Diken EG, Johnson MA (2009) Generating spectra from ground-state wave functions: Unraveling anharmonic effects in the $OH^-{\cdot}H_2O$ vibrational predissociation spectrum. *J Phys Chem* 113:7346–7352.
28. Corcelli SA, Skinner JL (2005) Infrared and Raman line shapes of dilute HOD in liquid H_2O and D_2O from 10 to 90 °C. *J Chem Phys* 109:6154–6165.
29. Schmidt JR, Corcelli SA, Skinner JL (2005) Pronounced non-Condon effects in the ultrafast infrared spectroscopy of water. *J Chem Phys* 123:044513.
30. Li S, Schmidt JR, Corcelli SA, Lawrence CP, Skinner JL (2006) Approaches for the calculation of vibrational frequencies in liquids: Comparison to benchmarks for azide/water clusters. *J Chem Phys* 124:204110.
31. Ufimtsev IS, Kalinichev AG, Martinez TJ, Kirkpatrick RJ (2007) A charged ring model for classical OH^-(aq) simulations. *Chem Phys Lett* 442:128–133.
32. Auer B, Kumar R, Schmidt JR, Skinner JL (2007) Hydrogen bonding and Raman, IR, and 2D-IR spectroscopy of dilute HOD in D_2O. *Proc Natl Acad Sci USA* 104:14215–14220.
33. Mitchell-Koch KR, Thompson WH (2008) Infrared spectra of a model phenol–amine proton transfer complex in nanoconfined CH_3Cl. *J Phys Chem B* 112:7448–7459.
34. Hanna G, Geva E (2008) Computational study of the one and two dimensional infrared spectra of a vibrational mode strongly coupled to its environment: Beyond the cumulant and Condon approximations. *J Phys Chem B* 114:12991–13004.
35. Schmidt JR, et al. (2007) Are water simulation models consistent with steady-state and ultrafast vibrational spectroscopy experiments? *Chem Phys* 341:143–157.
36. Mukamel S (1995) *Principles of Nonlinear Optical Spectroscopy* (Oxford Univ Press, New York).
37. Loparo JJ, Roberts ST, Nicodemus RA, Tokmakoff A (2007) Variation of the transition dipole moment across the stretching band of water. *Chem Phys* 341:218–229.
38. Diken EG, et al. (2005) Fundamental excitations of the shared proton in the $H_3O_2^-$ and $H_5O_2^+$ complexes. *J Phys Chem A* 109:1487–1490.
39. Geissler PL, Dellago C, Chandler D, Hutter J, Parrinello M (2001) Autoionization in liquid water. *Science* 291:2121–2124.
40. Eaves JD, et al. (2005) Hydrogen bonds in liquid water are broken only fleetingly. *Proc Natl Acad Sci USA* 102:13019–13022.
41. Loparo JJ, Roberts ST, Tokmakoff A (2006) Multidimensonal infrared spectroscopy of water. I. Vibrational dynamics in 2D lineshapes. *J Chem Phys* 125:194521.